



Contents lists available at ScienceDirect

Journal of Solid State Chemistry

journal homepage: www.elsevier.com/locate/jssc

A series of pure inorganic eight-connected self-catenated network based on Silverton-type polyoxometalate

Huaqiao Tan, Weilin Chen, Yang-Guang Li, Ding Liu, Limin Chen, Enbo Wang*

Key Laboratory of Polyoxometalate Science of the Ministry of Education, Department of Chemistry, Northeast Normal University, Renmin Street No.5268, Changchun Jilin 130024, PR China

ARTICLE INFO

Article history:

Received 29 July 2008

Received in revised form

20 October 2008

Accepted 3 November 2008

Available online 20 November 2008

Keywords:

Silverton-type polyoxometalate

Eight-connected self-catenated framework

Lanthanide metals

Transition metal

Crystal structure

ABSTRACT

In this paper, three pure inorganic eight-connected self-catenated networks based on the Silverton-type polyoxometalate $[\text{CeMo}_{12}\text{O}_{42}]^{8-}$ with lanthanide, transition metal and alkali metal cations as linkers: $[\text{Li}(\text{H}_2\text{O})_4]_2\text{Co}(\text{H}_2\text{O})_4\text{Ce}(\text{H}_2\text{O})_3[\text{CeMo}_{12}\text{O}_{42}] \cdot 3\text{H}_2\text{O}$ (**1**), $\text{H}_{0.5}[\text{Li}(\text{H}_2\text{O})_4]_{2.5}[\text{Ni}(\text{H}_2\text{O})_4]_{0.5}\text{Ce}(\text{H}_2\text{O})_3[\text{CeMo}_{12}\text{O}_{42}] \cdot 3\text{H}_2\text{O}$ (**2**) and $\text{H}[\text{Li}(\text{H}_2\text{O})_4]_3\text{Ce}(\text{H}_2\text{O})_3[\text{CeMo}_{12}\text{O}_{42}] \cdot 3\text{H}_2\text{O}$ (**3**) have been successfully synthesized and characterized by elemental analysis, IR spectroscopy, thermal gravimetric analysis, X-ray photoelectron spectroscopy, electrochemical analyses and single crystal X-ray diffraction. The single crystal X-ray diffraction analyses reveal that compounds **1–3** are isostructural. The $[\text{Ce}^{\text{IV}}\text{Mo}_{12}\text{O}_{42}]^{8-}$ polyoxoanions are connected by Ce^{4+} to form the infinite 1D chains. And then the parallel stacking chains linked by transition metal cations and lithium ions construct to an eight-connected self-catenated $4^{24}56^3$ topology framework.

© 2008 Elsevier Inc. All rights reserved.

1. Introduction

Entanglements observed commonly in catenanes, rotaxanes and molecular knots in the fields of biology have attracted considerable attention not only for their potential applications as functional solid materials but also for their intriguing architectures and topologies [1–4]. Recently, thanks to the eximious work of Robson, Ciani, Batten and others, many entangled networks have been obtained under a strategy of “network approach” [5,6]. However, the study of self-catenation nets, having the smallest topological rings catenated by other rings belonging to the same network, is still in its infancy. Until now, only a few self-catenated nets have been reported in metal-organic frameworks, implying a challenging issue in coordination chemistry [7,8].

Our group has great interest in entangled structures for a long time and successfully made a series of novel entangled structures: the interlocked and interdigitated architectures are synthesized by reaction of long flexible ligands and cadmium salts [9]; and a series of entangled coordination networks with inherent features of polycatenation, polythreading, and polyknotting obtained by self-assembly of the rigid 4,4'-bipyridine, the long V-shaped 4,4'-oxybis(benzoate) ligands and Ni^{2+} [10]. Based on our previous work of entangled coordination polymers, we wonder if such experience could be directed toward the design and synthesis of

novel pure inorganic entangled networks, since these inorganic materials have the true metal oxide surfaces and potential applications in different areas such as catalysis, ion exchange, sorption and molecular electronics [11].

Polyoxometalates (POMs), as an important family of metal-oxide clusters with plenty of structural topologies and a variety of physical and chemical properties [12–15], have been proved to be one of the most effective building block to construct entangled networks. Recently, many POMs-based entangled networks have been obtained [16], for example a three-connected fivefold interpenetrating network based on $[\text{PW}_{10}\text{W}_2\text{O}_{40}]^{5-}$ building blocks [17], and a fourfold interpenetrating 3D network constructed from the $\text{Cu}[\text{P}_4\text{Mo}_6\text{O}_{25}(\text{OH})_6]_2$ clusters and Cu-bpy groups have been reported [18]. However, most of the above compounds are low connected coordination frameworks (namely, connectivities less than six), and composed of polyoxoanions and organic linkers. The pure inorganic POMs-based entangled networks have reported scarcely, especially the highly connected coordination framework because of the limited coordination sites of metal centers and the steric hindrance of metal cations. Therefore, the synthesis of pure inorganic highly connected entangled networks is one of the most challenging issues in synthetic chemistry and material science. However, two strategies have been used to overcome these problems in synthesis of metal-organic frameworks at present. One is to take advantage of high coordination numbers and flexible coordination modes of lanthanide metals [19]. The other is the use of polynuclear metal clusters with large surface areas as building blocks, which can effectively reduce the steric hindrance of organic linkers [20]. Based on these

* Corresponding author. Fax: +86 431 85098787.

E-mail addresses: liyig658@nenu.edu.cn (Y.-G. Li),
wangeb889@nenu.edu.cn (E. Wang).

experiences, we investigate the reaction between the lanthanide cations and ball-type polyoxoanion $[\text{CeMo}_{12}\text{O}_{42}]^{8-}$, which has large surface areas and is stable in a wide pH range, aiming to construct the pure inorganic highly connected entangled networks.

Herein, we report the synthesis and character of three pure inorganic eight-connected self-catenated frameworks based on the Silverton-type POMs: $[\text{Li}(\text{H}_2\text{O})_4]_2\text{Co}(\text{H}_2\text{O})_4\text{Ce}(\text{H}_2\text{O})_3[\text{CeMo}_{12}\text{O}_{42}] \cdot 3\text{H}_2\text{O}$ (**1**), $\text{H}_{0.5}[\text{Li}(\text{H}_2\text{O})_4]_{2.5}[\text{Ni}(\text{H}_2\text{O})_4]_{0.5}\text{Ce}(\text{H}_2\text{O})_3[\text{CeMo}_{12}\text{O}_{42}] \cdot 3\text{H}_2\text{O}$ (**2**) and $\text{H}[\text{Li}(\text{H}_2\text{O})_4]_3\text{Ce}(\text{H}_2\text{O})_3[\text{CeMo}_{12}\text{O}_{42}] \cdot 3\text{H}_2\text{O}$ (**3**). The single crystal X-ray diffraction analyses reveal that compounds **1–3** are isostructural. The $[\text{Ce}^{\text{IV}}\text{Mo}_{12}\text{O}_{42}]^{8-}$ polyoxoanions are connected by Ce^{4+} to form the infinite 1D chains. And then the parallel stacking chains linked by transition metal cations and Li^+ construct to a unique eight-connected $4^{24}56^3$ topology framework, which is the first pure inorganic eight-connected self-catenated POMs-based network and the first 3D POMs-based extended materials with lanthanide and transition metal as linkers simultaneously.

2. Experimental section

2.1. General procedures

All reagents were commercially purchased and used without further purification. Elemental analyses (Ce, Li, Mo, Co, Ni) were determined by a PLASMA-SPEC(I) ICP atomic emission spectrometer. IR spectra were recorded in the range $400\text{--}4000\text{ cm}^{-1}$ on an Alpha Centaur FT/IR spectrophotometer using KBr pellets. TG analyses were performed on a Perkin-Elmer TGA7 instrument in flowing N_2 with a heating rate of $10^\circ\text{C min}^{-1}$. X-ray photoelectron spectroscopy (XPS) analyses were performed on a VGESCALABMKII spectrometer with an $\text{MgK}\alpha$ (1253.6 eV) achromatic X-ray source. The vacuum inside the analysis chamber was maintained at $6.2 \times 10^{-6}\text{ Pa}$ during the analysis. Electrochemical measurements were carried out on a CHI 600A electrochemical workstation at room temperature ($25\text{--}30^\circ\text{C}$) under nitrogen atmosphere.

2.2. Synthesis of compounds

Synthesis of 1: $(\text{NH}_4)_6\text{Mo}_7\text{O}_{24} \cdot 4\text{H}_2\text{O}$ (1.854 g, 1.5 mmol) was dissolved in 40 ml of water with stirring, the solution was heated to 90°C , a solution of $(\text{NH}_4)_2\text{Ce}(\text{NO}_3)_6$ (0.5480 g, 1 mmol) in water (20 ml) was added dropwise. When the reaction mixture was cooled to 65°C , a solution of 6 M H_2SO_4 (3 ml) was added. Keep at this temperature for 30 min. And then $\text{CoCl}_2 \cdot 6\text{H}_2\text{O}$ (1.1897 g, 5 mmol) and $\text{Li}_2\text{SO}_4 \cdot \text{H}_2\text{O}$ (0.6398 g, 5 mmol) were added. The final solution was heated to 80°C for 2 h, filtered. And the filtrate was kept for slow evaporation at room temperature. The orange block crystals of **1** were isolated after one week (yield 40%, based on Mo). Anal. Calcd for: $\text{H}_{36}\text{Li}_2\text{CoCe}_2\text{Mo}_{12}\text{O}_{60}$: Li, 0.55%; Co, 2.36%; Ce, 11.21%; Mo, 46.04%. Found: Li, 0.61%; Co, 2.44%; Ce, 11.13%; Mo, 45.98%.

Synthesis of 2: This compound was prepared similarly to **1**, with $\text{NiCl}_2 \cdot 6\text{H}_2\text{O}$ (1.1885 g, 5 mmol) instead of $\text{CoCl}_2 \cdot 6\text{H}_2\text{O}$. Lime block crystals were obtained from the solution after two weeks (yield 60%, based on Mo). Anal. Calcd for: $\text{H}_{36.5}\text{Li}_{2.5}\text{Ni}_{0.5}\text{Ce}_2\text{Mo}_{12}\text{O}_{60}$: Li, 0.70%; Ni, 1.19%; Ce, 11.32%; Mo, 46.51%. Found: Li, 0.75%; Ni, 1.23%; Ce, 11.29%; Mo, 46.45%.

Synthesis of 3: An identical procedure with **1** was followed to prepare **3** except that $\text{CoCl}_2 \cdot 6\text{H}_2\text{O}$ was not added. Yellow block crystals were obtained from the solution after two weeks (yield 75%, based on Mo). Anal. Calcd for: $\text{H}_{37}\text{Li}_3\text{Ce}_2\text{Mo}_{12}\text{O}_{60}$: Li, 0.85%; Ce, 11.44%; Mo, 47.00%. Found: Li, 0.91%; Ce, 11.38%; Mo, 46.98%.

2.3. X-ray crystallography

Single crystal X-ray data for compounds **1–3** were collected on a Rigaku R-Axis RAPID IP diffractometer equipped with a normal focus 18 kW sealed tube X-ray source ($\text{MoK}\alpha$ radiation, $\lambda = 0.71073\text{ \AA}$) operating at 50 kV and 200 mA. Data processing was accomplished with the RAXWISH processing program. A numerical absorption correction was applied. The structure was solved by direct methods and refined by full-matrix least-squares

Table 1
Crystal data and structure refinement for **1–3**.

	Compound 1	Compound 2	Compound 3
Empirical formula	$\text{H}_{36}\text{CoCe}_2\text{Li}_2\text{O}_{60}\text{Mo}_{12}$	$\text{H}_{36.5}\text{Ni}_{0.5}\text{Ce}_2\text{Li}_{2.5}\text{O}_{60}\text{Mo}_{12}$	$\text{H}_{37}\text{Ce}_2\text{Li}_3\text{O}_{60}\text{Mo}_{12}$
Formula mass	2500.62	2475.02	2449.64
Temperature (K)	293(2)	293(2)	293(2)
Wavelength (\AA)	0.71073	0.71073	0.71073
Crystal system	trigonal	trigonal	trigonal
Space group	$R\text{-}3c$	$R\text{-}3c$	$R\text{-}3c$
a (\AA)	18.568(3)	18.625(3)	18.610(3)
b (\AA)	18.568(3)	18.625(3)	18.610(3)
c (\AA)	24.088(5)	24.038(5)	24.037(5)
α (deg)	90.00	90.00	90.00
β (deg)	90.00	90.00	90.00
γ (deg)	120.00	120.00	120.00
V (\AA^3)	7192(2)	7222(2)	7209(2)
Z	6	6	6
D_{calcd} (g cm^{-3})	3.464	3.415	3.385
μ (mm^{-1})	5.355	5.190	5.009
$F(000)$	7014	6948	6876
Data/restraints/parameters	1783/1/118	1475/4/136	1755/1/141
Goodness-of-fit on F^2	1.178	1.006	1.194
R_1^a [$I > 2\sigma(I)$]	0.0345	0.0338	0.0170
wR_2^b	0.1014	0.0995	0.0508
Largest diff. peak and hole (e \AA^{-3})	1.036 and -2.219	1.232 and -1.316	0.537 and -0.570

^a $R_1 = \sum ||F_o| - |F_c|| / \sum |F_o|$.

^b $wR_2 = \sum [w(F_o^2 - F_c^2)^2] / \sum [w(F_o^2)^2]^{1/2}$.

on F^2 using the SHELXL 97 software [21,22]. All the non-hydrogen atoms were refined anisotropically. A summary of the crystallographic data and structure refinement for compounds **1–3** are given in Table 1. Further details of the crystal structure investigations of **1–3** may be obtained from the Fachinformationszentrum Karlsruhe, D-76344 Eggenstein-Leopoldshafen, Germany (E-mail: Crysdata@fiz-karlsruhe.de) on quoting the deposited numbers CSD-419567 for **1**, CSD-419568 for **2** and CSD-419569 for **3**.

3. Result and discussion

3.1. Crystal structure of compounds

Single crystal X-ray diffraction analyses reveal that compounds **1–3** are isostructural. **1** is described as an example below. Compound **1** is built from dodecamolybdocates(IV) $[\text{Ce}^{\text{IV}}\text{Mo}_{12}\text{O}_{42}]^{8-}$ polyoxoanions, which belongs to the Silverton-type polyoxometalate: $[\text{MMo}_{12}\text{O}_{42}]^{n-}$ ($M = \text{Ce}^{\text{IV}}, \text{U}^{\text{IV}}, \text{Zr}^{\text{IV}}, \text{Th}^{\text{IV}}, \text{Np}^{\text{IV}}, n = 8; M = \text{Gd}^{\text{III}}, \text{Ce}^{\text{III}}, n = 9$). It can be described as a central CeO_{12} icosahedron surrounded by six face-shared MoO_9 units linked together by corner-sharing with Ce–O bond lengths of 2.486–2.494 Å and Mo–O bond lengths of 1.697–2.330 Å. Recently, in POMs-based extended materials the commonly used POM building blocks are still limited to well-known Keggin- [23], Wells-Dawson- [24], Anderson- [25] and Lindquist-type [26] anions et al. The research about the polyoxoanions $[\text{Ce}^{\text{IV}}\text{Mo}_{12}\text{O}_{42}]^{8-}$ remains scarce [27–29].

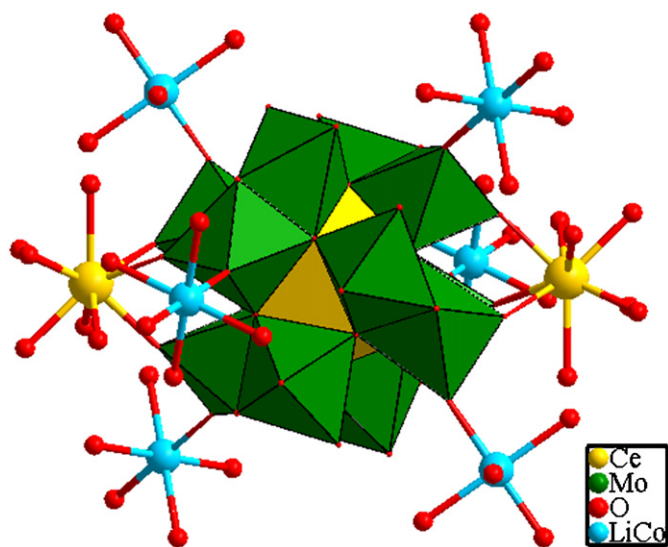


Fig. 1. The combined polyhedral and ball-and-stick presentation of **1**.

In compound **1**, the $[\text{Ce}^{\text{IV}}\text{Mo}_{12}\text{O}_{42}]^{8-}$ clusters act as polydentate ligands coordinating to two $\text{Ce}(2)^{4+}$, two Co^{2+} and four Li^+ through terminal oxygen atoms (Fig. 1). Each Ce (2) ion in **1** is coordinated by three water molecules and six terminal oxygen atoms from two $[\text{Ce}^{\text{IV}}\text{Mo}_{12}\text{O}_{42}]^{8-}$ polyoxoanions (Ce(2)– O_w 2.518 Å; Ce(2)– O_t 2.341 Å). The polyoxoanions are interconnected through $[\text{Ce}(\text{H}_2\text{O})_3]^{4+}$ bridging groups to form an infinite 1D chain, as shown in Fig. 2. And then the parallel stacking chains are linked by six metal cations to form a 3D framework (Fig. 3). It is noteworthy that six metal centers exhibit the site-occupancy disorder with 1/3 of Co and 2/3 of Li, respectively. Each metal cation is a distorted octahedron formed by four water molecules ($M\text{--O}_w$, 2.288–2.324 Å) and two terminal oxygen atoms from two $[\text{Ce}^{\text{IV}}\text{Mo}_{12}\text{O}_{42}]^{8-}$ polyoxoanions ($M\text{--O}$, 2.093–2.095 Å) [30]. The 3D POMs-based framework which is constructed from polyoxoanions with lanthanide and transition metal cations as linkers simultaneously has never been observed.

Further, from the topological point of view, the $[\text{Ce}^{\text{IV}}\text{Mo}_{12}\text{O}_{42}]^{8-}$ polyoxoanion can be abstracted as an eight-connected node which links with two $\text{Ce}(2)^{4+}$, two Co^{2+} and four Li^+ . The $\text{Ce}(2)^{4+}$, Co^{2+} and Li^+ linkers can be viewed as a two-connected node which connected with two $[\text{Ce}^{\text{IV}}\text{Mo}_{12}\text{O}_{42}]^{8-}$ clusters. Thus the 3D framework of **1** can be abstracted into a unique eight-connected $4^{24}5^{63}$ topology net (Fig. 4).

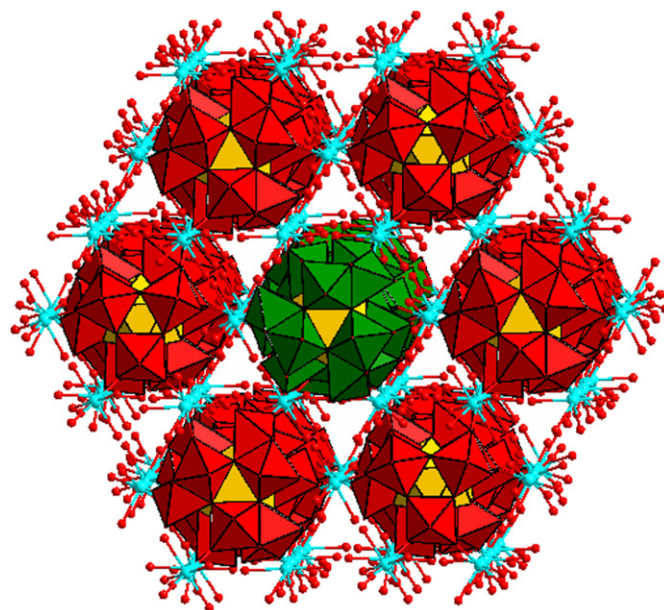


Fig. 3. The 3D framework structure of **1** as a combined polyhedral and ball-and-stick representation.

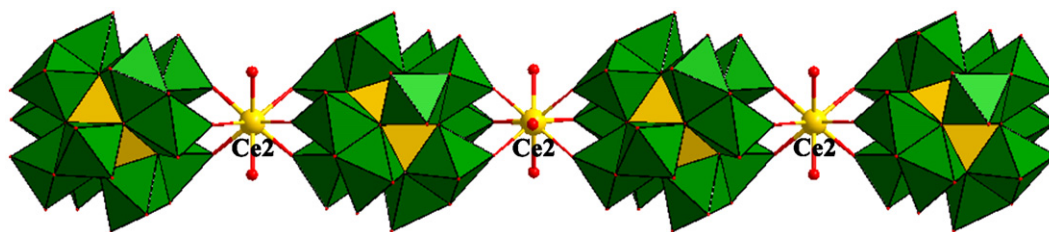


Fig. 2. The 1D chain structure constructed from the $[\text{Ce}^{\text{IV}}\text{Mo}_{12}\text{O}_{42}]^{8-}$ polyoxoanions connected by $\text{Ce}(2)^{4+}$.

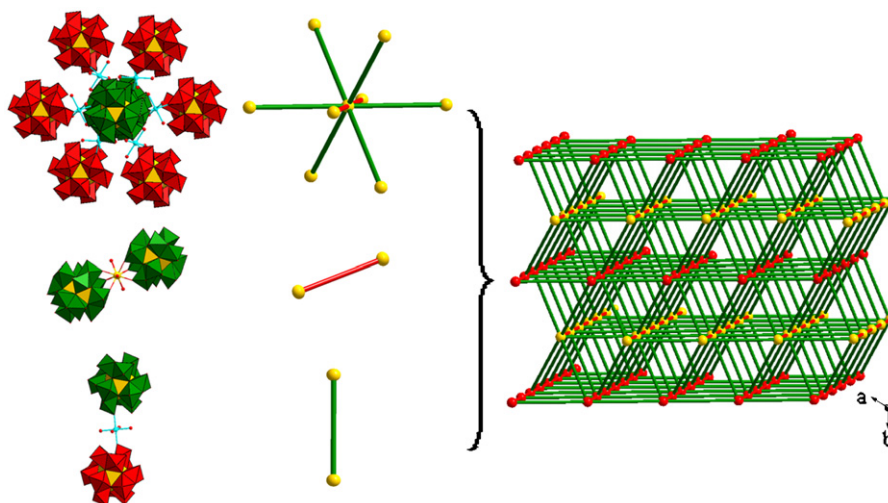


Fig. 4. Topological representation of **1** showing the $4^{24}56^3$ topology.

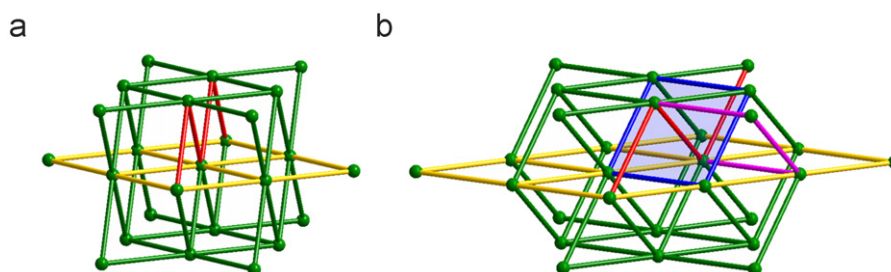


Fig. 5. Schematic representations illustrating the different links between the 4^4 nets in the eight-connected nets of bcu (a) and **1** (b). The self-penetrating shortest circuits are highlighted.

Notably, the structure of **1** is completely different from that of the familiar body-centered cubic lattice (bcu) [31]. As shown in Fig. 5, the parallel (4,4) nets (yellow) of both bcu and **1** are crosslinked by zigzag chains (red); however, the detailed connection modes are different. In bcu, the red zigzag chain in the interlayer region bridges across the diagonal of a single window in the (4,4) net (Fig. 5a). In **1**, however, it bridges the diagonal of two windows (Fig. 5b). As a result of this unique bridging of parallel layers, the catenated four-membered shortest rings are observed at the intersection of the crossing of 2D layers. Therefore, the resulting array is a single eight-connected self-catenated network (Fig. 4).

Up to date, only three eight-connected self-catenated structures have been reported. Our group first reported the two compounds: $[\text{Zn}_5(\mu_3\text{-OH})_2(\text{bdc})_4(\text{phen})_2]$ (phen = 1,10-phenanthroline) with $4^{24}56^3$ topology [32] and $[\text{Cd}_3(\text{bdc})_3(\text{L})_2(\text{H}_2\text{O})_2]$ [L = 1,4-bis(1,2,4-triazol-1-yl)butane and bdc = 1,4-benzenedicarboxylate] with $4^{20}6^8$ topology [33]. Recently, Xu and co-workers have reported the third compound: $[\text{Cu}_4(\text{bpp})_4\text{V}_4\text{O}_{12}] \cdot 3\text{H}_2\text{O}$ [bpp = 1,3-bis(4-pyridyl)propane] with $4^{24}6^4$ topology [19]. But all of the above compounds are composed of polynuclear metal clusters and organic linkers. Therefore, compound **1** is the first eight-connected self-catenated POMs-based network, which composed of pure inorganic compounds.

The framework structure in **2** and **3** are essentially isomorphous to that observed in **1** with the exception that the

constituent $\{\text{Ce}^{\text{IV}}\text{Mo}_{12}\text{O}_{42}\}_n$ chains are interconnected by one $\{\text{Ni}(\text{H}_2\text{O})_4\}$ and five $\{\text{Li}(\text{H}_2\text{O})_4\}$ bridging groups in **2**, and six $\{\text{Li}(\text{H}_2\text{O})_4\}$ bridging groups in **3**.

3.2. IR and UV-vis spectroscopy

In the IR spectrum of compound **1**, the peaks at 3153 and 1616 cm^{-1} are assigned to OH stretching and scissoring. Vibration modes at 958, 823, 593 and 409 cm^{-1} were attributed to $\nu(\text{Mo}=\text{O}_t)$, $\nu(\text{Mo}-\text{O}-\text{Mo})$, $\nu(\text{Mo}-\text{O}-\text{Ce}, \text{Mo})$ and $\nu(\text{Ce}-\text{O})$, respectively, (see Fig. S4). The UV-vis spectra of compounds **1–3** in aqueous (see Figs. S1–3) exhibit two main peaks in the region of 239–240 nm and the range of 345–362 nm, attributable to the $\text{O} \rightarrow \text{Mo}$ charge transition [11]. The absorption values at 400 nm might be originated from the $\text{O} \rightarrow \text{Ce}$ charge transition.

3.3. X-ray photoelectron spectroscopy

XPS was performed to identify the existence and oxidation states of Ce, Co, Ni in compounds **1** and **2**. Fig. 6a shows the XPS spectrum of **1** in Ce 3d region with peaks at 905.2 and 888.4 eV ascribed to Ce^{4+} , while compound **2** exhibits a similar XPS curve in Ce 3d region with peaks at 905.5 and 886.7 eV ascribed to Ce^{4+} too, shown in Fig. 6c. Fig. 6b shows the spectrum of **1** in Co 2p region with a peak at 784.9 eV attributed to Co^{2+} , and in Fig. 6d, the XPS

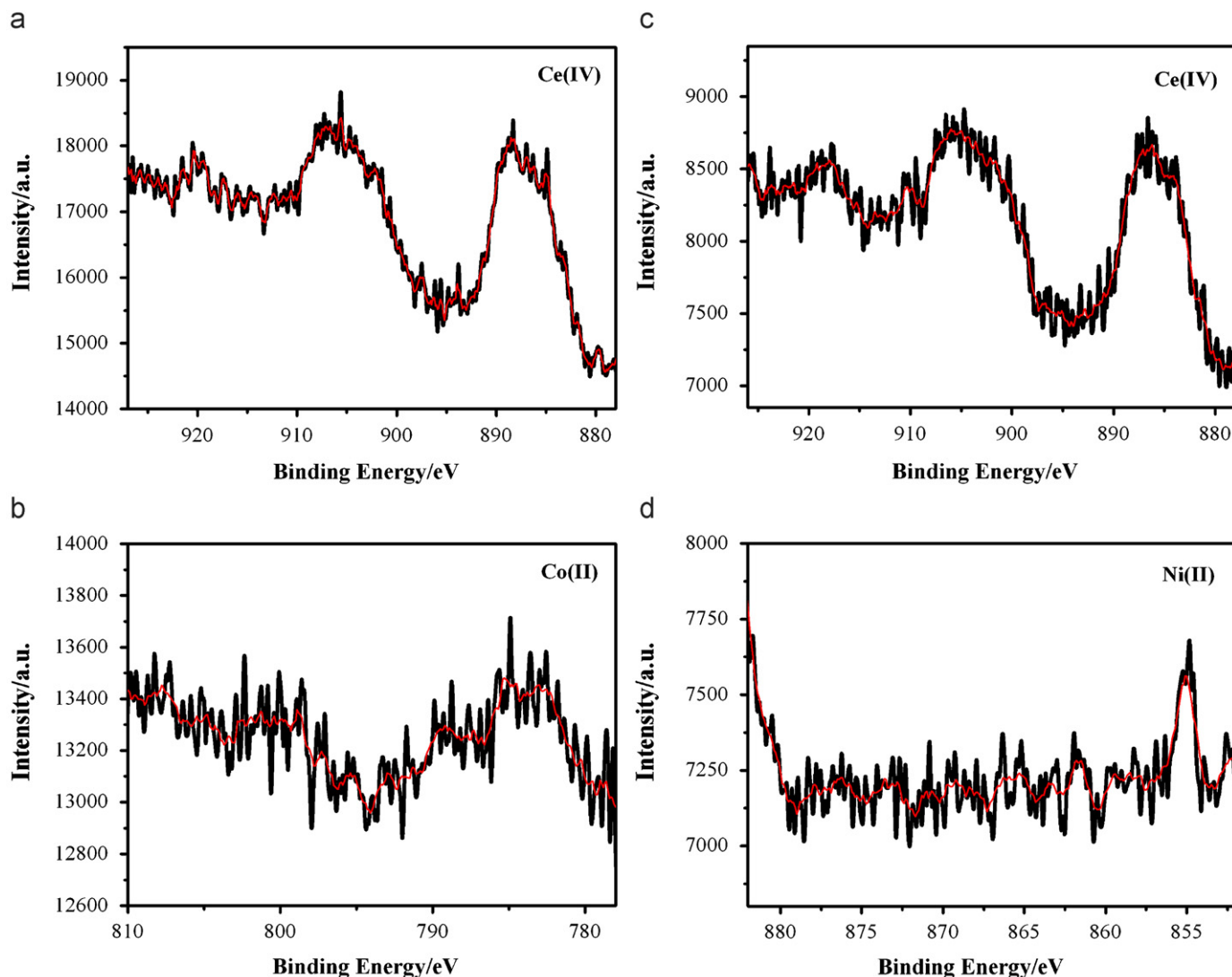


Fig. 6. (a) XPS spectrum of Ce^{4+} of **1**; (b) XPS spectrum of Co^{2+} of **1**; (c) XPS spectrum of Ce^{4+} of **2**; (d) XPS spectrum of Ni^{2+} of **2**.

curve with a peak at 855.1 eV is owed to the Ni^{2+} of compound **2**. The XPS estimation of the valence-state values seems to be in reasonable agreement with those calculated from the bond valence sum calculations.

3.4. Electrochemical properties

Compound **1–3** are insoluble in the solution of 1 M Na_2SO_4 at room temperature. Therefore, the electrochemical behavior of compounds **1**-, **2**- and **3**-modified carbon paste electrode were investigated in pH = 2 (1 M $\text{H}_2\text{SO}_4 + \text{Na}_2\text{SO}_4$) buffer solution at the scan rate of 25 mV s^{-1} . The three compounds exhibit similar electrochemical behaviors except for some displacements. The CV of **1** (see Fig. 7a) possesses two irreversible redox pairs at $E_{1/2} = +0.015$ and $+0.146 \text{ V}$ [$E_{1/2} = (E_{\text{pa}} + E_{\text{pc}})/2$], which are responsible for redox processes of Mo^{VI} . Another irreversible peak at $+1.093 \text{ V}$ should correspond to the redox process of Ce(IV)/Ce(III) [34]. The CV of **2** (see Fig. 7b) displays three irreversible redox pairs at $E_{1/2} = +0.015$, $+0.245$ and $+0.480 \text{ V}$, attributed to redox

processes of the polyoxomolybdate. Further, it also exhibits one irreversible redox pairs at $+1.113 \text{ V}$, ascribed to a Ce(IV)/Ce(III) redox process [34]. In the CV of **3** (Fig. 7c), there are also three irreversible redox peaks at $E_{1/2} = +0.012$, $+0.159$ and $+0.378 \text{ V}$, which are ascribed to redox processes of Mo^{VI} , while the irreversible redox peak at $+1.109 \text{ V}$ is attributed to the Ce(IV)/Ce(III) redox process.

4. Conclusion

In summary, we have synthesized three new 3D extended frameworks based on $[\text{Ce}^{\text{IV}}\text{Mo}_{12}\text{O}_{42}]^{8-}$ polyoxoanions. The $[\text{Ce}^{\text{IV}}\text{Mo}_{12}\text{O}_{42}]^{8-}$ clusters are connected by lanthanide, transition metal and alkali metal cations simultaneously to form a unique 3D $4^{24}56^3$ topology net. The compounds are the first eight-connected self-catenated POMs-based network, which are composed of pure inorganic compounds. And it is also the first 3D example that polyoxoanions are connected by lanthanide and transition metal simultaneously.

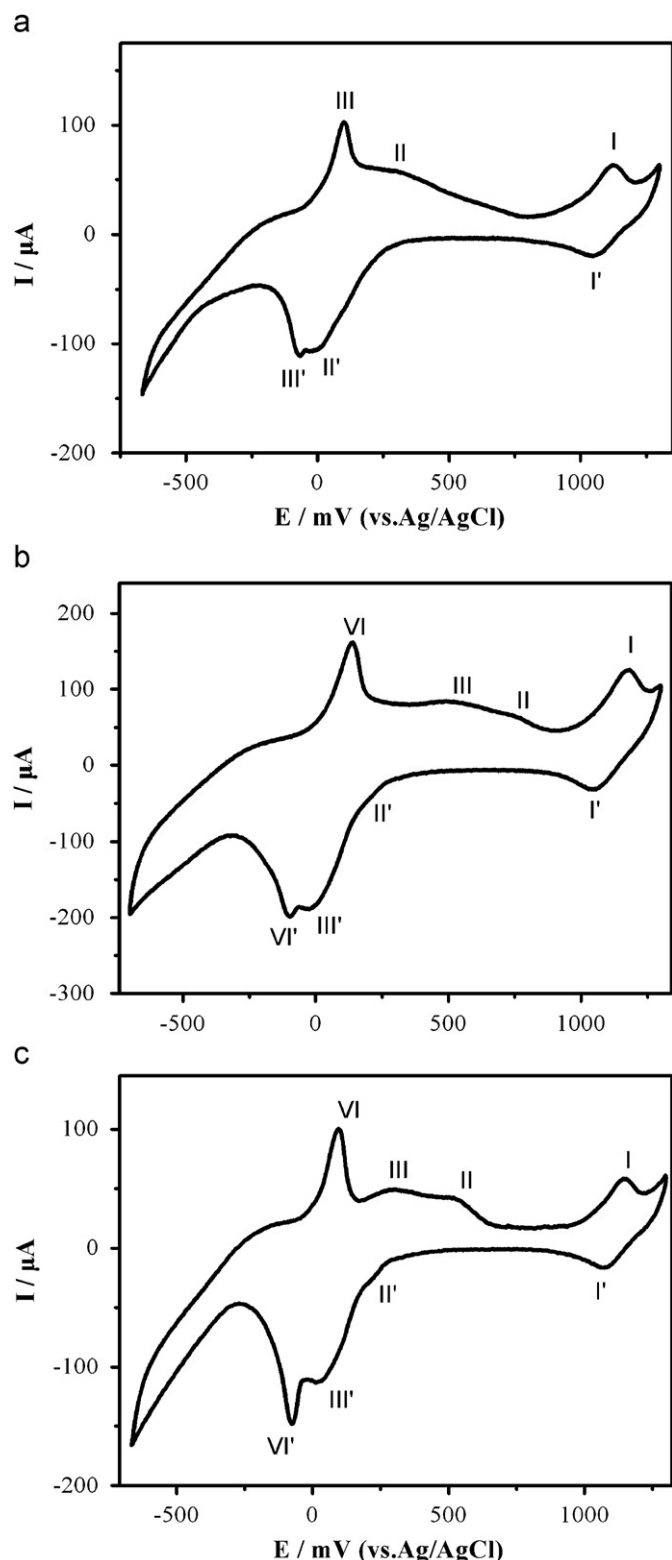


Fig. 7. Cyclic voltammogram of compound **1(a)**, **2(b)** and **3(c)** in the 1 M $\text{H}_2\text{SO}_4\text{--Na}_2\text{SO}_4$ aqueous solution at the scan rate of 25 mV s^{-1} .

Acknowledgments

This work was supported by the National Natural Science Foundation of China (no. 20701005/20701006); the Science and

Technology Development Project Foundation of Jilin Province (no. 20060420); the Postdoctoral Station Foundation of Ministry of Education (no. 20060200002); the Testing Foundation of Northeast Normal University (NENU); Science and Technology Creation Foundation of NENU (NENU-STC07009) and Science Foundation for Young Teachers of NENU (no. 20070302/20070312); the Program for Changjiang Scholars and Innovative Research Team in University; the Program for National Innovative Research of Chinese students.

Appendix A. Supporting Information

Supplementary data associated with this article can be found in the online version at doi:10.1016/j.jssc.2008.11.011.

Text6References

- [1] J.P. Sauvage, C. Dietrich-Buchecker, *Molecular Catenanes, Rotaxanes and Knots*, A Journey Through the World of Molecular Topology, Wiley, Weinheim, 1999.
- [2] S.R. Batten, R. Robson, *Angew. Chem. Int. Ed.* 37 (1998) 1460–1494.
- [3] S.R. Batten, *Cryst. Eng. Commun.* 3 (2001) 67–72.
- [4] L. Carlucci, G. Ciani, D.M. Proserpio, *Coord. Chem. Rev.* 246 (2003) 247–289.
- [5] S.A. Bourne, J. Lu, B. Moulton, M.J. Zaworotko, *Chem. Commun.* (2001) 861–862.
- [6] X.H. Bu, M.L. Tong, H.C. Chang, S. Kitagawa, S.R. Batten, *Angew. Chem. Int. Ed.* 43 (2004) 192–195.
- [7] P. Jensen, D.J. Price, S.R. Batten, B. Moubarki, K.S. Murray, *Chem. Eur. J.* 6 (2000) 3186–3195.
- [8] L. Carlucci, G. Ciani, D.M. Proserpio, F. Porta, *Angew. Chem. Int. Ed.* 42 (2003) 317–322.
- [9] X.L. Wang, C. Qin, E.B. Wang, L. Xu, Z.M. Su, C.W. Hu, *Angew. Chem. Int. Ed.* 43 (2004) 5036–5040.
- [10] X.L. Wang, C. Qin, E.B. Wang, Y.G. Li, Z.M. Su, L. Xu, *Angew. Chem. Int. Ed.* 44 (2005) 5824–5827.
- [11] M.T. Pope, *Heteropoly and Isopoly Oxometalates*, Springer, Berlin, 1983.
- [12] C.L. Hill, *Chem. Rev.* 98 (1998) 1–3.
- [13] L.C. Baker, D.C. Glick, *Chem. Rev.* 98 (1998) 3–50.
- [14] D.L. Long, E. Burkholder, L. Cronin, *Chem. Soc. Rev.* 36 (2007) 105–121.
- [15] E. Coronado, G. García, *Chem. Rev.* 98 (1998) 273–296.
- [16] C. Streb, C. Ritchie, D.L. Long, P. Kögerler, L. Cronin, *Angew. Chem. Int. Ed.* 46 (2007) 7579–7582.
- [17] L.L. Fan, D.R. Xiao, E.B. Wang, Y.G. Li, Z.M. Su, X.L. Wang, *Cryst. Growth Des.* 7 (2007) 592–594.
- [18] J. Liu, E.B. Wang, X.L. Wang, D.R. Xiao, L.L. Fan, *J. Mol. Struct.* 876 (2008) 206–210.
- [19] D.L. Long, R.J. Hill, A.L. Blake, N.P. Champness, P. Hubberstey, D.M. Proserpio, C. Wilson, M. Schröder, *Angew. Chem. Int. Ed.* 43 (2004) 1851–1854.
- [20] X.S. Qu, L. Xu, G.G. Gao, F.Y. Li, Y.Y. Yang, *Inorg. Chem.* 46 (2007) 4775–4777.
- [21] G.M. Sheldrick, *SHELXS97*, Program for Crystal Structure Solution, University of Göttingen, Germany, 1997.
- [22] G.M. Sheldrick, *SHELXL97*, Program for Crystal Structure Refinement, University of Göttingen, Germany, 1997.
- [23] M. Sadakane, M.H. Dickman, M.T. Pope, *Angew. Chem. Int. Ed.* 39 (2000) 2914–2916.
- [24] J.Y. Niu, D.J. Guo, J.P. Wang, J.W. Zhao, *Cryst. Growth Des.* 4 (2004) 241–247.
- [25] V. Shivaiah, P.V.N. Reddy, L. Cronin, S.K. Das, *J. Chem. Soc. Dalton Trans.* (2002) 3781–3782.
- [26] D. Hagrman, P.J. Hagrman, J. Zubieta, *Angew. Chem. Int. Ed.* 38 (1999) 3165–3168.
- [27] L.C.W. Baker, G.A. Gallagher, T.P. Mccutcheon, *J. Am. Chem. Soc.* 75 (1953) 2493–2495.
- [28] V.N. Molchanov, I.V. Tat'yanina, E.A. Torchenkova, *Chem. Commun.* (1981) 93–94.
- [29] C.D. Wu, C.Z. Lu, H.H. Zuang, J.S. Huang, *J. Am. Chem. Soc.* 124 (2002) 3836–3837.
- [30] R. Boulatov, B. Du, E.A. Meyers, S.G. Shore, *Inorg. Chem.* 38 (1999) 4554–4558.
- [31] O.D. Friedrichs, M. ORKeeffe, O.M. Yaghi, *Acta Crystallogr. Sect. A* 59 (2003) 22–28.
- [32] X.L. Wang, C. Qin, E.B. Wang, Z.M. Su, X. Lin, S.R. Batten, *Chem. Commun.* (2005) 4789–4791.
- [33] X.L. Wang, C. Qin, E.B. Wang, Z.M. Su, *Chem. Eur. J.* 12 (2006) 2680–2691.
- [34] W.L. Chen, Y.G. Li, Y.H. Wang, E.B. Wang, Z.M. Su, *Dalton Trans.* (2007) 4293–4301.